Ultrafast Spin-Motion Entanglement and Interferometry with a Single Atom

C. Senko,[1,*] J. Mizrahi,[1] W. C. Campbell,[1] K. G. Johnson,[1] C. W. S. Conover,[2] and C. Monroe[1]

[1] *Joint Quantum Institute, University of Maryland Department of Physics and National Institute of Standards and Technology, College Park, Maryland 20742*

[2] *Colby College Physics Department, Waterville, Maine 04901*

(Dated: February 1, 2012)

We report entanglement of a single atom's hyperfine spin state with its motional state on a timescale of order 15 ns. We engineer a short train of intense laser pulses to impart a spin-dependent momentum transfer of $\pm 2\hbar k$. We further create an atomic interferometer using pairs of momentum kicks and demonstrate collapse and revival of spin coherence as the motional wavepacket is split and recombined. The revival after a pair of kicks occurs only when the second kick is delayed by an integer multiple of the period of the harmonic trap, a signature of entanglement and disentanglement of the spin with the motion. Such quantum control may allow a new regime of ultrafast entanglement between atomic qubits.

Trapped atomic ions are a leading platform for quantum information processing, with a well-developed toolkit for coherent manipulations [1], including deterministic spin-spin interactions mediated by transitory spin-motion entanglement. These tools have been used to experimentally demonstrate quantum algorithms [2, 3], multiparticle entanglement [4, 5], and quantum simulations [6, 7], among other advances. To date, most coherent manipulations of trapped ions are performed in the weak excitation regime, wherein the interaction between the ions and the laser fields is characterized by a Rabi frequency Ω that is smaller than the motional trap frequency ω_t. Recent work has demonstrated coherent spin flips in the strong excitation regime, $\Omega \gg \omega_t$ [8], using picosecond laser pulses [9] and near-field microwave gradients [10], but motional control has not been observed in the strong excitation limit. Here we realize ultrafast spin-motion entanglement, using a short train of picosecond pulses from a mode-locked laser to drive stimulated Raman transitions. The resulting spin-state-dependent momentum transfer occurs in an interaction time under 15 ns, nearly two orders of magnitude faster than the trap oscillation period of 1.26 μs. Such spin-dependent kicks are a key building block for fast entanglement of multiple ion qubits via the Coulomb interaction [11, 12]. These entangling gates, in contrast to motional gates using spectroscopically resolved sidebands, may be performed faster than a trap oscillation period, and are thereby less sensitive to slow noise and more easily scaled to large crystals of ions within a single trap [13].

In addition to entangling gates, other applications of impulsive spin-dependent kicks include fast sideband cooling [14] or interferometry [8]. Our technique of building up a velocity kick out of several scattering pulses similar to the Kapitza-Dirac pulses first demonstrated in [15] allows the atomic wavepacket to be resolved into two motional states with high fidelity, an advantage of using Bragg scattering, while still retaining certain advantages of the Raman-Nath scattering regime such as short interaction time and insensitivity to initial momentum [16].

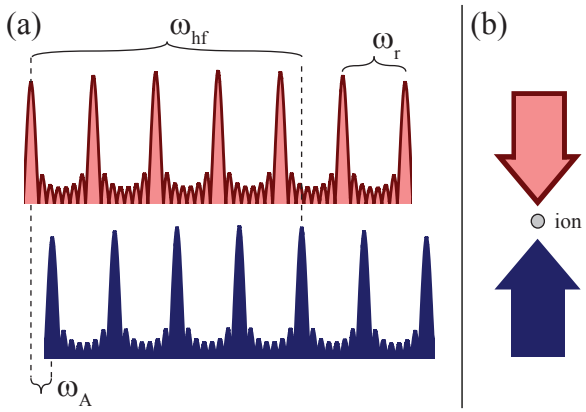

FIG. 1. (color online) (a): Sketch of the optical spectrum seen by the ion for generating a spin-dependent momentum kick when Eq. (1) is satisfied. (b): Depiction of the wavevectors associated with the spectra in (a). An atom starting in the $|\downarrow\rangle$ state may be driven to the $|\uparrow\rangle$ state only by absorbing a photon from the blue (solid) beam and emitting a photon into the red (lightly shaded) beam, resulting in a momentum transfer of $2\hbar k$ in the upward direction. Similarly, an atom starting in the $|\uparrow\rangle$ state may only make a transition such that it receives $2\hbar k$ momentum in the downward direction.

In this work, we demonstrate a small-scale interferometer by separating pairs of impulsive kicks by integer multiples of the trap oscillation period, analogous to atomic interferometers with trap evolution playing the role of the atomic reflectors [17].

To understand how a pair of short pulse trains can effect a spin-dependent momentum kick, we first consider the spectrum of each pulse train. As sketched in Fig. 1, we apply counterpropagating frequency combs with a relative frequency shift to the ion in order to drive stimulated Raman transitions between the hyperfine levels representing the effective spin. The resulting spectrum is such that a spin state can only undergo a transition by absorbing a photon from one beam and emitting a photon into the other beam, with the roles of the beams reversed for the other spin state. In order for this process

Report Documentation Page

Form Approved
OMB No. 0704-0188

1. REPORT DATE	2. REPORT TYPE	3. DATES COVERED
01 FEB 2012		**00-00-2012 to 00-00-2012**

4. TITLE AND SUBTITLE	5a. CONTRACT NUMBER
Ultrafast Spin-Motion Entanglement and Interferometry with a Single Atom	5b. GRANT NUMBER
	5c. PROGRAM ELEMENT NUMBER
6. AUTHOR(S)	5d. PROJECT NUMBER
	5e. TASK NUMBER
	5f. WORK UNIT NUMBER
7. PERFORMING ORGANIZATION NAME(S) AND ADDRESS(ES) **University of Maryland,Joint Quantum Institute,Department of Physics and National Institute of Standards and Technology,College Park,MD,20742**	8. PERFORMING ORGANIZATION REPORT NUMBER
9. SPONSORING/MONITORING AGENCY NAME(S) AND ADDRESS(ES)	10. SPONSOR/MONITOR'S ACRONYM(S)
	11. SPONSOR/MONITOR'S REPORT NUMBER(S)

12. DISTRIBUTION/AVAILABILITY STATEMENT
Approved for public release; distribution unlimited

13. SUPPLEMENTARY NOTES

14. ABSTRACT

15. SUBJECT TERMS

16. SECURITY CLASSIFICATION OF:			17. LIMITATION OF ABSTRACT	18. NUMBER OF PAGES	19a. NAME OF RESPONSIBLE PERSON
a. REPORT **unclassified**	b. ABSTRACT **unclassified**	c. THIS PAGE **unclassified**	**Same as Report (SAR)**	**4**	

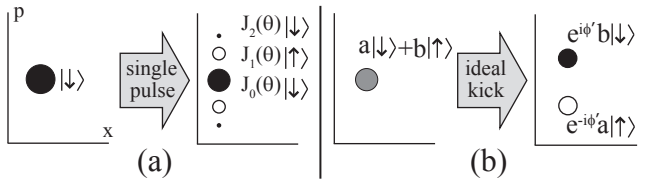

FIG. 2. Phase-space illustration of the different forms of spin-motion entanglement accessible in the strong-excitation regime. (a): Effect of applying a single counterpropagating pulse pair in the lin⊥lin polarization configuration. The initial wavepacket is diffracted into momentum states separated by $2n\hbar k$ whose amplitude, $J_n(\theta)$, is given by the strength of the scattering pulse; a spin flip occurs for each of the odd-n orders. (b): Effect of applying an ideal "spin-dependent kick" pulse train. The initial wavepacket is split into two momentum states entangled with the spin.

to occur, the two beams must have spectral components separated by the hyperfine frequency ω_{hf}, i.e.

$$\omega_{hf} = n\omega_r \pm \omega_A, \tag{1}$$

where n is an integer, ω_r the repetition rate of the pulse train, and ω_A the relative frequency shift imparted by acousto-optic modulators (AOMs). This is the same condition necessary to drive a carrier transition in the resolved sideband limit [18]. However, here the momentum transfer due to a π pulse is nearly instantaneous compared to the trap evolution, so that rather than leaving the motional state unaffected, a spin-dependent impulse excites all of the motional sidebands simultaneously. Since we do not wish to kick both spin states in both directions, the width of the comb "teeth" must be narrower than the shift ω_A, and ω_{hf} may not be an integer or half-integer multiple of ω_r. The key to performing a spin-dependent kick is thus to create a pair of frequency combs of sufficient intensity, subject to these requirements, in a time much shorter than the trap period.

To understand the process described above in terms of a sequence of discrete scattering pulses, we first consider the effects of a single counterpropagating pulse pair with simultaneous arrival times and orthogonal linear polarizations. In our system, linearly polarized light cannot drive Raman transitions; the polarization gradient therefore creates a standing wave in the Rabi frequency, resulting in the Hamiltonian (setting $\hbar = 1$):

$$H(t) = \omega_t a^\dagger a + \frac{\omega_{hf}}{2}\sigma_z + \frac{\Omega(t)}{2}\sin\left(\eta(a^\dagger + a) + \phi(t)\right)\sigma_x, \tag{2}$$

where a and $a^\dagger$ are the ladder operators of the harmonic motional mode along the standing wave field, $\Omega(t)$ is the time-varying Rabi frequency, η is the Lamb-Dicke parameter, and $\phi(t) = \omega_A t + \phi_0$ is the phase of the standing wave. Since the pulse is extremely short, we can approximate $\Omega(t) \approx \theta\delta(t - t_0)$, and directly integrate the Hamiltonian to obtain the evolution operator for the pulse pair arriving at time t_0:

$$U_{p,t_0} = \sum_{n=-\infty}^{\infty} e^{in\phi(t_0)} J_n(\theta)\mathcal{D}(in\eta)\sigma_x^n, \tag{3}$$

where we have assumed that the effects of hyperfine evolution and trap evolution are negligible during the pulse. This behavior, illustrated in Fig. 2(a), is as expected for a Kapitza-Dirac scattering pulse [15]. The problem of setting the delays between several pulses such that population coherently accumulates in only the momentum orders of interest is somewhat reminiscent of the temporal Talbot effect seen in matter waves [19], but is complicated by the entanglement of the various momentum states with the spin.

An analysis similar to that described in [18] shows that a train of such pulses may be used to generate a spin-dependent momentum kick, in which the spin states receive respective displacements in phase space of exactly $\pm i\eta$. The previous work, in order to neglect contributions from all but one of the motional sidebands, assumes the pulse train is much longer than a trap period and the ions are strongly confined in the Lamb-Dicke regime. By contrast, we need not remain within the Lamb-Dicke regime; we instead assume a pulse train much shorter than a trap period, such that trap evolution is negligible during the pulse sequence. Under this assumption, the evolution operator for m pulses spaced by a time T becomes

$$O_m = U_{p,(m-1)T} e^{i\omega_{hf}T\sigma_z/2} \cdots U_{p,T} e^{i\omega_{hf}T\sigma_z/2} U_{p,0}. \tag{4}$$

In the limit of many pulses with a total pulse area of π (i.e. $\theta = \pi/m$ for each pulse) and under the condition in Eq. (1), the effect of this pulse sequence converges to the ideal operator (illustrated in Fig. 2(b)),

$$U_{SDK} = e^{i\phi'}\mathcal{D}(i\eta)\sigma_\mp + e^{-i\phi'}\mathcal{D}(-i\eta)\sigma_\pm, \tag{5}$$

where $\phi' = \phi_0 \pm m\omega_{hf}T/2$ and the signs in ϕ' and of the raising and lowering operators are chosen to agree with the sign in Eq. (1). In practice, with as few as four pulses the operator Eq. (4) approximates the evolution described in Eq. (5) with better than 90% fidelity, as we have checked with numerical simulations.

The experimental setup is shown in Fig. 3. A $^{171}Yb^+$ ion is confined in a linear four-rod Paul trap and the hyperfine "clock states" of its $^2S_{1/2}$ ground manifold, split by $\omega_{hf}/2\pi = 12.642815$ GHz, are used as the spin states, $|\downarrow\rangle \equiv |F = 0, m_F = 0\rangle$ and $|\uparrow\rangle \equiv |F = 1, m_F = 0\rangle$. Light near resonant with the $^2S_{1/2} \longleftrightarrow {}^2P_{1/2}$ transition at 369 nm is used to perform Doppler cooling, state preparation, and state detection [20]. The Raman pulse trains are derived from a picosecond mode-locked frequency-tripled vanadate laser that generates an average power of 3.5 W at 355 nm. This wavelength, detuned by 33 THz from the nearest excited state, is near an optimum

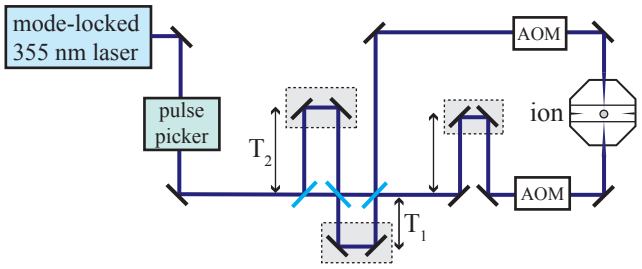

FIG. 3. (color online) Experimental schematic showing the pulsed laser beam path, including pulse-shaping interferometers for splitting each pulse into a four-pulse sequence, and variable delays for tailoring the spectrum of the four-pulse train (T_1, T_2) and for matching the arrival times of the counterpropagating pulses.

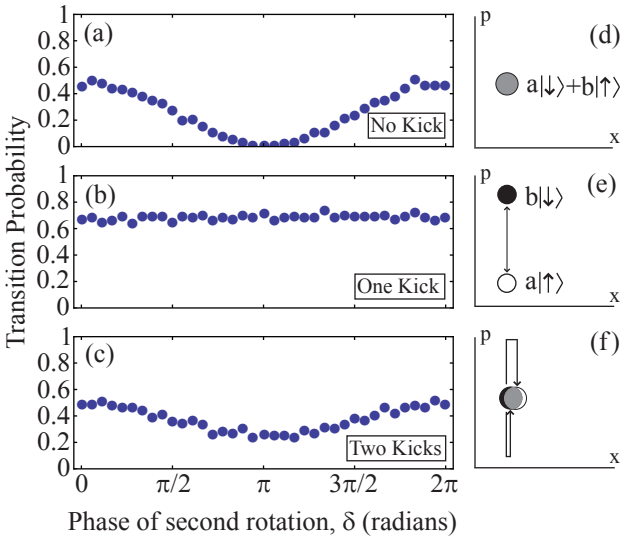

FIG. 4. (color online) Results from scanning the phase of the final rotation in the experimental sequence $R_\delta(\alpha)U_{SDK}R_0(\alpha)$, where $R_\delta(\alpha)$ represents a rotation on the Bloch sphere by an angle α about the axis $e^{-i\delta}\sigma_+ + e^{i\delta}\sigma_-$. The choice of $\alpha = \pi/4$ is due to limitations imposed by our low trap frequency and large Lamb-Dicke parameter. The data shown are for U_{SDK} representing (a) the identity (no kicking pulses), (b) a single spin-dependent kick comprising an 8-pulse train, and (c) two consecutive kicking 8-pulse trains; (d)-(f) sketch the idealized phase-space evolution due to U_{SDK} in each case. The loss of contrast after a single kick and its reappearance after a second kick are a hallmark that the kicks entangle and disentangle the spin with the motion.

for minimizing spontaneous emission from the P states and first-order differential AC Stark shifts [9]. The duration of each pulse is $\tau \approx 10$ ps with a repetition rate of 80.1533 MHz. The repetition rate is stabilized via a piezo mounted on one of the oscillator cavity mirrors using a PID servo loop driven by the output of a fast photodiode signal mixed with a local oscillator at 80.1533 MHz [18]. An electro-optic pulse picker is used to extract individual pulses from the beam that are sent through the delay interferometers described below, frequency-shifted with AOMs, and focused onto the ion. The counterpropagating pulse trains are directed along the quantization axis (defined by a magnetic field of 3 G), nearly parallel to one of the principal axes of the trap, with orthogonal linear polarizations and their path lengths are equalized to much better than $c/\tau \approx 3$ mm to match their arrival times. Resolved-sideband Raman spectroscopy verifies that the laser field couples mainly to a single transverse mode at $\omega_t/2\pi = 795$ kHz, with a residual coupling to the 70 kHz axial mode due to a slight misalignment.

In order to obtain the desired spin-selectivity in the direction of momentum transfer, a spectrum comprising several pulses is required; however, trap evolution over the duration of even a four-pulse train from the laser would interfere with the production of the spin-dependent kick. We therefore create a pulse train of shorter duration using a pulse-shaping scheme consisting of concatenated Mach-Zehnder interferometers with imbalanced arm lengths, which splits each pulse from the laser into a train of four pulses with tunable relative delays, as shown in Fig. 3. Since we perform both strong-pulse and resolved-sideband operations using the same beam path, the repetition rate of this pulse train and that of the laser must both satisfy Eq. (1) with the same sign. Subject to this restriction, the AOMs generate a frequency offset between the two beams of $\omega_A/2\pi = 422$ MHz, which limits the allowable delay between each of the four pulses to $T = 2\pi n/(\omega_{hf} + \omega_A)$, where n is any integer. However, we must also account for the reflective phase shift introduced by the beam splitters: specifically, a pulse pair that originally traveled through the short arm of the final delay interferometer will have a phase shift of π relative to a pulse pair that traveled through the long arm. To compensate for this, the final delay is set such that n is a half-integer, specifically $n = 11/2$ (corresponding to a delay of $T_1 = 421$ ps), while the initial delay is unaffected by this phase shift and remains set to $n = 10$. Splitting the pulse further in this manner will reduce the infidelity exponentially with the number of added interferometers. For example, based on numerical evaluation of Eq. (4) we predict a fidelity of 91% for the four-pulse train reported here, but an eight- or sixteen-pulse train would improve the fidelity to 97.5% or 99%, respectively, while imposing a modest price in terms of experimental complexity.

We produce a spin-dependent kick using two successive pulses from the laser, creating an eight-pulse train of duration 13.7 ns, to achieve an integrated pulse area of roughly π. The expected gain in fidelity due to the additional pulses is offset by the extra trap evolution, and we measure a population transfer probability from $|\downarrow\rangle$ to $|\uparrow\rangle$ of 89% due to one such eight-pulse kick. Since we cannot probe the motion directly, we study the spin coherence by performing rotations on the Bloch sphere

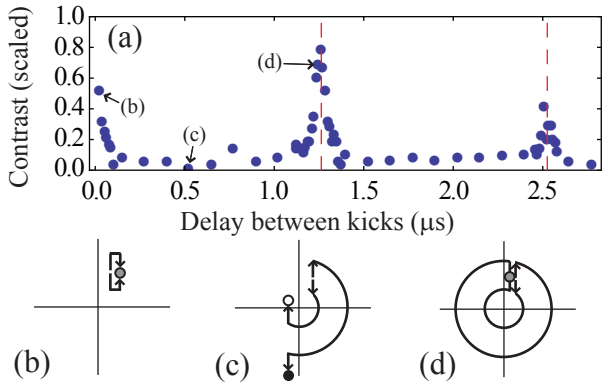

FIG. 5. (color online) (a): Plot of contrast versus the delay between two spin-dependent kicks. The contrast at each point is obtained from the amplitude of a sinusoidal fit to a dataset similar to the ones presented in Figure 4, and is scaled to the contrast obtained with no spin-dependent kicks (Figure 4(a)). Red dashed lines indicate the duration of 1 and 2 cycles of the 795 kHz transverse mode. (b)-(d): Sketches of the phase-space evolution at the kick separations indicated in (a).

before and after the spin-dependent kicks and measuring the contrast obtained by varying the axis of the final rotation. The contrast would be expected to disappear and reappear as the spin-dependent kicks cause the motional wavepacket to be split and recombined in phase space, as is seen in Fig. 4. Furthermore, were the motional state independent of the spin, a single kick would not cause the loss of contrast seen in Fig. 4(b), whereas the revival of coherence seen due to a second kick in Fig. 4(c) demonstrates that the decay of contrast is not due to some other decoherence process. These scans therefore provide indirect confirmation that we are entangling the spin state with the motion.

A further demonstration of motional involvement in this process is provided by studying the contrast after a pair of spin-dependent kicks as a function of the delay between the kicks. As seen in Fig. 5, the contrast revival decays as the second kick is delayed and the separated wavepackets evolve to different positions, such that a pure momentum transfer is insufficient to recombine the motional wavepackets in phase space. Revival is then seen again when the delay is near an integer multiple of a trap period and the spin states are again in the same position, though due to the directionality of the momentum transfer, such a revival is not expected at half-integer multiples of the trap period. The degradation of the contrast revival at two trap cycles compared to one is likely due to a 1-2 degree misalignment of the laser beams allowing a slight coupling to the 70 kHz axial mode. The clear signature of revival with precisely the same period as the trap provides further confirmation that we are successfully entangling and disentangling the spin with the motional state.

We have demonstrated ultrafast entanglement of an atom's spin and motion in an experimental regime that has remained largely unexplored, and used pairs of our spin-dependent kicks to create an interferometer. We anticipate that a 9 W Raman laser will allow a spin-dependent kick to be performed by splitting a single laser pulse into a pulse train of duration 1.2 ns, representing an order of magnitude speedup in the kick duration. Future work will explore the application of multiple kicks from alternating directions, increasing the area enclosed by the interferometer. In addition to improving the sensitivity of interferometric measurements, this will increase the amount of conditional phase imprinted on a pair of ions exposed to these kicks, allowing the generation of a fast controlled-phase-flip entangling gate. For example, with the 9 W Raman laser and a weaker trap, a protocol similar to [12] could be performed in a time much shorter than the motional period.

This work is supported by grants from the U.S. Army Research Office with funding from the DARPA OLE program, IARPA, and the MURI program; the NSF PIF Program; the NSF Physics Frontier Center at JQI; and the European Commission AQUTE program.

* csenko@umd.edu

[1] R. Blatt and D. Wineland, Nature **453**, 1008 (2008).
[2] S. Guld *et al.*, Nature **421**, 48 (2003).
[3] K.-A. Brickman *et al.*, Phys. Rev. A **72**, 050306 (2005).
[4] C. A. Sackett *et al.*, Nature **404**, 256 (2000).
[5] T. Monz *et al.*, Phys. Rev. Lett. **106**, 130506 (2011).
[6] R. Islam *et al.*, Nature Communications **2**, 377 (2011).
[7] J. T. Barreiro *et al.*, Nature **470**, 486 (2011).
[8] J. F. Poyatos *et al.*, Phys. Rev. A **54**, 1532 (1996).
[9] W. C. Campbell *et al.*, Phys. Rev. Lett. **105**, 090502 (2010).
[10] C. Ospelkaus *et al.*, Nature **476**, 181 (2011).
[11] J. J. Garcia-Ripoll, P. Zoller, and J. I. Cirac, Phys. Rev. Lett. **91**, 157901 (2003).
[12] L.-M. Duan, Phys. Rev. Lett. **93**, 100502 (2004).
[13] S.-L. Zhu, C. Monroe, and L.-M. Duan, Europhysics Letters **73**, 485 (2006).
[14] S. Machnes *et al.*, Phys. Rev. Lett. **104**, 183001 (2010).
[15] P. L. Gould, G. A. Ruff, and D. E. Pritchard, Phys. Rev. Lett. **56**, 827 (1986).
[16] R. E. Sapiro, R. Zhang, and G. Raithel, Phys. Rev. A **79**, 043630 (2009).
[17] M. Kasevich and S. Chu, Phys. Rev. Lett. **67**, 181 (1991).
[18] D. Hayes *et al.*, Phys. Rev. Lett. **104**, 140501 (2010).
[19] L. Deng *et al.*, Phys. Rev. Lett. **83**, 5407 (1999).
[20] S. Olmschenk *et al.*, Phys. Rev. A **76**, 052314 (2007).